An Energy-Efficient Resource Access Scheme in NOMA Heterogeneous Wireless Communication Systems

N. Keshava
Department of EECE, GITAM (Deemed to be University), Bengaluru Campus, India | Department of ECE, Cambridge Institute of Technology North Campus, VTU, India
keshavan_1212@rediffmail.com (corresponding author)

M. Ramesha
Department of Electrical, Electronics and Communication Engineering, GITAM (Deemed to be University), Bengaluru Campus, India
rameshmalur037@gmail.com

Received: 7 May 2025 | Revised: 10 August 2025 | Accepted: 22 August 2025

 DOI: https://doi.org/10.48084/etasr.11975

ABSTRACT

This research explores the potential of Multi-Input Multi-Output Non-Orthogonal Multiple Access (MIMO-NOMA) within the framework of 5G and 6G wireless communication networks. Recognizing the critical role of NOMA in enhancing connectivity and spectral efficiency, this study focuses on addressing the challenge of resource allocation in MIMO-NOMA environments. To optimize throughput while minimizing energy consumption, a novel State-Action Game-based Energy Efficient Resource Allocation Optimization (SAG-EERAO) model is introduced. This model effectively accommodates real-world challenges such as imperfect Channel State Information (CSI), mobility, and dynamic throughput requirements. The proposed SAG-EERAO framework is assessed within an urban-highway interference environment, demonstrating its robustness and adaptableness. Comparative performance evaluations indicate that SAG-EERAO surpasses existing approaches by significantly reducing energy consumption, improving spectrum utilization efficiency, and enhancing throughput. This study provides innovative perspectives and practical advancements in the deployment and optimization of MIMO-NOMA, underscoring the effectiveness of SAG-based methodologies for dynamic and efficient resource management in next-generation wireless communication systems.

Keywords-Deep Reinforcement Learning (DRL); energy efficiency; game theory; Multi-Input Multi-Output (MIMO); Non-Orthogonal Multiple Access (NOMA); power optimization; resource access; State-Action Game (SAG)

I. INTRODUCTION

Non-Orthogonal Multiple Access (NOMA) has gained significant attention as a promising multiple access technique in the evolution of 5G and beyond (6G) wireless networks, as discussed in [1]. Unlike traditional Orthogonal Multiple Access (OMA) schemes, where users are assigned separate time-frequency resources [2], NOMA allows multiple users to share the same resources simultaneously, significantly enhancing spectral efficiency, system capacity, and user connectivity [3]. One of the primary advantages of NOMA is its ability to handle interference more efficiently than OMA systems [3, 4]. While traditional OMA schemes suffer from low spectral utilization due to strict orthogonal allocation [5], NOMA leverages power domain multiplexing for concurrent transmissions [6]. Successive Interference Cancellation (SIC) at the receiver helps to separate and decode signals [7].

The integration of Multiple Input Multiple Output (MIMO) with NOMA (MIMO-NOMA) amplifies these benefits by improving spatial diversity and throughput [5]. However, power allocation among users in MIMO-NOMA systems remains a critical challenge [6]. Effective power allocation is essential for ensuring fairness, system efficiency, and Quality of Service (QoS), all while addressing channel conditions and interference. Channel State Information (CSI) plays a vital role in optimizing resource allocation [7], yet perfect CSI is hard to achieve due to estimation errors and SIC imperfections. Many studies still assume ideal CSI [3, 6], which results in suboptimal performance in practical scenarios [8].

Imperfect CSI in real-world NOMA deployments can degrade service quality, especially for users with poor channel conditions. Moreover, factors such as user mobility [9], energy consumption [10], and urban multipath fading [11] further challenge NOMA's effectiveness. Despite its potential, much existing research overlooks these real-world complexities.

To address these limitations, reinforcement learning-based models, especially State-Action Game (SAG) approaches such as game theory and Deep Reinforcement Learning (DRL), have been explored for optimizing resource allocation in NOMA systems [12, 13]. SAG models offer a dynamic framework to manage user interactions and adapt resource strategies in real time. This paper introduces a novel SAG-based Energy Efficient Resource Allocation Optimization (SAG-EERAO) approach for large-scale MIMO-NOMA networks. It addresses key concerns including imperfect SIC, CSI errors, fairness, mobility, and energy efficiency. The contributions of this work are as follows:

- A novel MIMO-NOMA resource access design is introduced using a SAG model to maximize throughput while minimizing energy consumption.
- A utility function is optimized by considering user cooperation in MIMO-NOMA.
- The model is tested under complex urban propagation environments.
- Compared with existing methods, the SAG-based optimization significantly improves spectrum efficiency and energy usage.

Several related works have proposed diverse solutions for enhancing NOMA system performance. Authors in [14] employed user grouping based on channel gain differences and used a Deep Neural Network (DNN) for power allocation among subcarriers to maximize the system's sum rate. However, this assumes ideal conditions, ignoring SIC errors and inter-carrier interference. Authors in [15] proposed a modified DenStream evolutionary algorithm to dynamically cluster users, achieving uniform transmission rates but without addressing power allocation, a key component of overall efficiency. Authors in [16] introduced a joint optimization strategy for power and channel allocation in NOMA, balancing user fairness and system capacity. Though effective, the model's computational complexity limits real-time application. Authors in [17] proposed a strategy to boost energy efficiency by optimizing transmission schemes and resource usage. Although energy efficiency was improved, it required additional hardware, which may not be practical for all implementations. Authors in [18] integrated blockchain with NOMA-based Mobile Edge Computing (MEC) to jointly manage offloading, user clustering, and resource allocation. Though effective in reducing energy consumption, blockchain-induced computational overhead can counteract energy savings. Authors in [19] designed an online adaptive user and power allocation algorithm for dynamic MEC-NOMA networks. While improving throughput and latency, the approach can degrade under highly volatile conditions.

Game theory has also been applied in resource management. Authors in [20] proposed a Delta-OMA scheme using game theory for Visible Light Communication (VLC) networks. The model focused on fairness and capacity but added complexity, limiting its practical deployment. Authors in [21] addressed energy efficiency in a cell-free massive MIMO network, coexisting with a primary network. Using the Dinkelbach's algorithm and weighted MMSE, they presented a robust downlink power allocation model while addressing interference constraints. Authors in [22] proposed a delay-aware scheduling scheme for single-hop wireless networks, targeting applications with stringent delay requirements. The problem was modeled using delay-laxity and solved via a DRL approach based on Double Deep Q Networks (DDQN), outperforming conventional Q-learning in terms of reward and convergence rate. Authors in [23] focused on optimizing User Perceived Throughput (UPT) in Industrial Internet of Things (IIoT) environments. Their framework included joint MAC-layer scheduling and PHY-layer beamforming. Using Lyapunov optimization, they broke a long-term UPT problem into short-term subproblems. Their centralized and decentralized algorithms, using Fractional Programming (FP) and Successive Convex Approximation (SCA), showed superior UPT gains.

Authors in [24] highlighted the domain shift problem between simulated and real-world DRL models. They proposed a hybrid framework using digital twins and online DRL. The digital twin, built via behavior cloning, helped parameterize default policies in real environments. Their approach achieved up to 26.39% better resource utilization than conventional DRL, while maintaining system revenue. Authors in [25] introduced a Coherent Ising Machine (CIM)-based approach to optimize resource and channel allocation in NOMA systems. Built on mutually-connected photonic neural networks, CIM outperformed traditional optimization methods, especially in achieving fairness. Authors in [26] proposed a comprehensive model that includes sub-channel allocation, optimal base-station selection, and power reduction through DRL. A Deep Deterministic Policy Gradient (DDPG) approach was used, demonstrating superior sum-rate and power efficiency. Authors in [27] presented a Least-Subcarrier Sum-Gain-based User Assignment (LSSGUA) method for multi-carrier NOMA, along with intra- and inter-user power allocation. Their approach used worst sub-carrier first allocation and iterative bisection methods. Results showed improvements in spectral efficiency, fairness, outage probability, and overall sum-rate. Finally, authors in [28] showed that rational Low-Power Node (LPN) deployment in heterogeneous networks improves energy efficiency. However, their work used an OMA-based framework, lacking the spectral efficiency potential of NOMA systems [29].

In summary, while existing research demonstrates promising strategies for optimizing power, spectrum, and user fairness in NOMA, many models assume ideal conditions, overlook real-world challenges (e.g., mobility, imperfect CSI), or introduce high complexity. Thus, there remains a gap in developing lightweight, adaptive, and energy-efficient models [30] for large-scale deployment in dynamic environments. In the next section, we introduce a SAG-based EERAO framework that addresses these limitations and enhances the practical applicability of MIMO-NOMA systems.

II. PROPOSED METHODOLOGY

In this work, we examine a massive-NOMA system where the Base Station (BS) transmitters overlay information obtained from N users within a single subcarrier, contrasting with a multi-carrier OMA system where information from an individual user is sent across every subcarrier. The transmitted signal through BS can be represented using Base-Band Unit (BBU) signals as:

$$y_o = \frac{1}{\sqrt{O}} \sum_{l=1}^{L} \left(\sum_{n=1}^{N} \sqrt{\beta_{l,n} Q_l B_{l,n}} \right) e^{-k\frac{2n}{O}} \quad (1)$$

where $0 \leq o \leq N-1$, L represents the total number of sub-carriers symbols within MIMO-NOMA, N represents the super-imposed users present in each sub-carrier, O represents both time-domain and frequency-domain in MIMO-NOMA, $B_{l,n}$ represents the n^{th} user data in the l^{th} sub-carrier, Q_l is the assigned-power for the l^{th} sub-carrier, and $\beta_{l,n}$ is the power allocation ratio for the n^{th} user in the l^{th} sub-carrier, as shown in Figure 1.

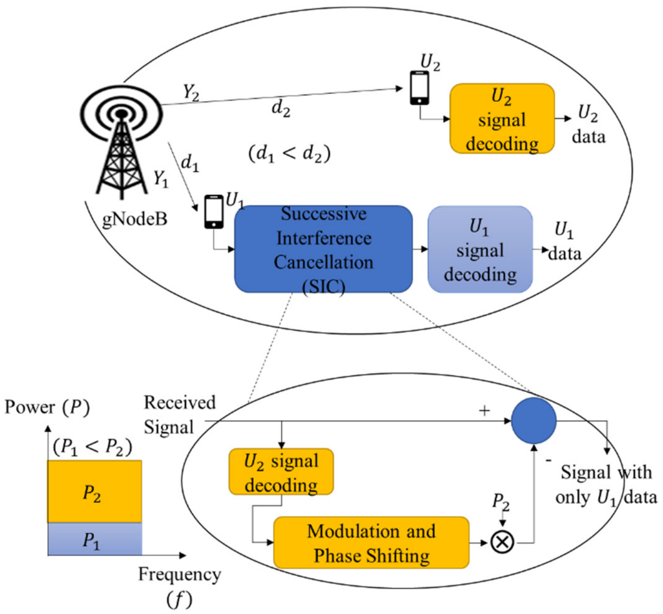

Fig. 1. Power allocation to Mobile Terminals (MTs) in a massive NOMA system.

To prevent interference among sub-carrier symbols within MIMO-NOMA, in this work, sub-carriers near the edge of the MIMO-NOMA 5G network are set as zero, and only selected sub-carriers are used for transmitting data. Let L_E denote the total sub-carriers used for transmitting data and total sub-carriers not used for transmitting be denoted as $(L - L_E)$. The $(L - L_E)$ are set as null which helps to provide security for bands near the edge of MIMO-NOMA 5G networks and sub-carriers transmitting data. For efficient subcarrier allocation, reducing power consumption and improving throughput, the signal from the MT is considered as a vector B_l, which is processed using an Inverse Fast Fourier-Transform (IFFT):

$$B_l = \sum_{n=1}^{N} B_{l,n} \quad (2)$$

When the Nyquist-Shannon rate equals the sampling frequency or the signal is oversampled M times, then $O = L$ in (1). Oversampling is achieved by inserting $(M-1)L$ zeroes in B_l before the IFFT process. Moreover, $\beta_{l,n}$ changes inversely with the user channel gain in a fast-fading scenario. Hence, users are arranged based on β values, from near to far, i.e., $\beta_{l,1} < \cdots < \beta_{l,n}$. The received signal for the n^{th} user on the l^{th} sub-carrier is:

$$Z_{l,n} = I_{l,n} \left(\sum_{n=1}^{N} \sqrt{\beta_{l,n} Q_l B_{l,n}} \right) + O_{l,n},$$
$$1 \leq l \leq L, \ 1 \leq n \leq N \quad (3)$$

In (3), $O_{l,n}$ represents Additive White Gaussian-Noise (AWGN) for the n^{th} on the l^{th} sub-carrier, with variance σ_n^α, and $I_{l,n}$ represents the channel-frequency-response between the BS and the n^{th} user, evaluated as:

$$I_{l,n} = \frac{h_{l,n}}{\sqrt{1+d_n^\alpha}} \quad (4)$$

where d_n^α represents the distance between the BS and n^{th} user, α represents the path-loss exponent, and $h_{l,n}$ represents the fast-fading parameter.

To mitigate interference from superimposed users, SIC is used at the receiver to isolate and eliminate interference, thereby allowing each user to extract its signal, as shown in Figure 2.

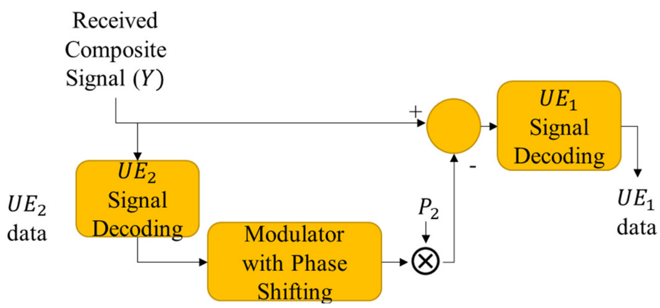

Fig. 2. SIC at the receiver of UE1 in a two-user-per-cluster NOMA system.

The extraction process is performed by sequentially subtracting the signals decoded for weak users (i.e., user j such that $j > n$) from the received signal of the n^{th} user. Moreover, interference in this work refers to the signals from strong users (i.e., user j such that $j < n$). During transmission, such interference may prevent efficient data transmission by the subcarriers. Therefore, (5) is used to evaluate the optimal data transmission rate for every n^{th} user on each sub-carrier:

$$S_n = \sum_{l=1}^{L} \log_2 (1 + \delta_{l,n}) \quad (5)$$

where:

$$\delta_{l,n} = \frac{Q_l |I_{l,n}|^2 \beta_{l,n}}{\left(Q_l |I_{l,n}|^2 \sum_{j=1}^{n-1} \beta_{l,n}\right) + \sigma_{l,n}^2} = \frac{Q_l |I_{l,n}|^2 \beta_{l,n}}{\left(Q_l |I_{l,n}|^2 \sum_{j=1}^{n-1} \beta_{l,n}\right) + 1} \quad (6)$$

In (6), $\delta_{l,n}$ denotes the Signal-to-Interference-plus-Noise Ratio (SINR) and $\tau_{l,n} \cong Q_l / \sigma_{l,n}^2$ denotes the Signal-to-Noise Ratio (SNR) for the n^{th} user on its respective l^{th} sub-carrier.

Moreover, in (6), the denominator converges towards zero when $\delta_{l,1}$, corresponding to the n^{th} user located near the BS. Equation (6) enables higher throughput with an optimal data transmission rate, and the total throughput considering SINR and SNR is evaluated using (7):

$$S_{l,n} = \sum_{n=1}^{N} S_n$$

$$= \sum_{n=1}^{N} \log_2 \prod_{l=1}^{L} \left(1 + C \frac{\tau_l |I_{l,n}|^2 \beta_{l,n}}{\left(\tau_l |I_{l,n}|^2 \sum_{j=1}^{n-1} \beta_{l,n}\right)+1}\right) \quad (7)$$

In Eq. (7), C denotes an optimized constant that assists in optimizing resource allocation for signal data transmission. The overall throughput is calculated using (8):

$$S_{TOTAL} = \sum_l \sum_{n=1}^{n/2-1} S_{l,n} \quad (8)$$

As (8) involves resource access, it increases energy consumption while providing decent throughput during signal transmission. Therefore, it is important to improve performance by maximizing throughput while minimizing energy consumption under urban-highway interference scenarios. To achieve this, the EERAO approach uses the SAG concept, which enhances throughput and reduces power usage in urban multipath fast-fading scenarios.

In this SAG-based framework, the model considers user coordination and the relationship between BSs and user group x. The utility function is used to select the best contender, and its value for each BS is evaluated using (9) and (10):

$$U_1^o = \varphi * S_1^o + \omega * C_3^\tau - \mu * C_3^\tau \quad (9)$$

$$U_2^o = \varphi * S_2^o + \omega * C_3^\rho - \mu * C_3^\rho \quad (10)$$

where φ and ω denote unit throughput and power overhead, C_3^τ and C_3^ρ represent the power allocated from BS_1 and BS_2, and μ is the objective-cost parameter:

$$\mu = y + z\left(C_3^\tau + C_3^\rho\right)^\alpha \quad (11)$$

where α, y, and z are non-negative constants, with $\alpha \geq 1$ ensuring convexity of the objective-cost parameter. Equation (11) indicates that BS cost increases as users consume more power. To reduce overall power consumption, BS_2 increases its utility by allocating more power to all connected users, thereby reducing cost for BS_1. This approach allows BS_1 to have higher power allocation when selecting resources compared with BS_2. As there is a trade-off between throughput and power, it is important to quantify this trade-off, which is done using (12):

$$q_3 \propto \frac{1}{C_3^\tau + C_3^\rho} \quad (12)$$

Equation (12) is further simplified as shown in the following equations:

$$\left[O_0 + H_{3B_1} q_3\right] = \frac{a_1}{C_3^\tau} \quad (13)$$

$$\left[O_0 + H_{3B_2} q_3\right] = \frac{a_2}{C_3^\rho} \quad (14)$$

In (13) and (14), a_1 and a_2 are non-negative constants. Using (9) and (10), (13) and (14) can be simplified to (15) and (16), respectively:

$$V_1^o = \varphi S_1^o + \omega C_3^\tau - \left[y + z\left(C_3^\tau + C_3^\rho\right)^\alpha\right] C_3^\tau \quad (15)$$

$$V_2^o = \varphi S_2^o + \omega C_3^\rho - \left[y + z\left(C_3^\tau + C_3^\rho\right)^\alpha\right] C_3^\rho \quad (16)$$

Considering (15) and (16), the optimal solution for efficient power-allocation for every group x is formulated as:

$$\max V_n^o\left(C_3^\tau + C_3^\rho\right) \quad (17)$$

subject to $C_\downarrow \leq C_3^\tau + C_3^\rho \leq C_\uparrow$, $0 \leq C_3^\tau \leq C_1$, $0 \leq C_3^\rho \leq C_2$, $\varphi, \omega, y, z > 0$, $a_1, a_2 \geq 0$, and $\alpha \geq 1$.

In (17), $C_\downarrow$ and $C_\uparrow$ denote the minimum and maximum bandwidth required for user coordination (i.e., pairing). The parameter $C_\downarrow$ helps control power transmission to reduce interference among BSs and user group x. This ensures that the selected NOMA channel resources for x do not exceed the allocated power, satisfying $0 \leq C_3^\tau \leq C_1$ and $0 \leq C_3^\rho \leq C_2$. By considering contenders and the Nash equilibrium, the optimal power allocation strategy is evaluated using:

$$\left(\hat{C}_3^\tau, \hat{C}_3^\rho\right) = arg \max V_n^o\left(C_3^\tau, C_3^\rho\right) \quad (18)$$

subject to the same constraints as in (17). To achieve the optimal Nash equilibrium for (15) and (16) in the SAG framework, V_n^o is adjusted with respect to C_3^τ and C_3^ρ. From this, (15) and (16) are modified into (19), representing the best strategy for selecting resources with minimal power allocation:

$$\begin{cases} \frac{\partial V_1^o(C_3^\tau, C_3^\rho)}{\partial V_3^\tau} = 0 \\ \frac{\partial V_2^o(C_3^\tau, C_3^\rho)}{\partial V_3^\rho} = 0 \\ 0 \leq C_3^\tau \leq C_1 \\ 0 \leq C_3^\rho \leq C_2 \\ C_\downarrow \leq C_3^\tau \leq C_3^\rho \leq C_\uparrow \end{cases} \quad (19)$$

The proposed SAG-based resource access model effectively allocates resources to mobile nodes with enhanced energy efficiency, higher throughput, and improved overall system performance.

III. SIMULATION STUDY

This section evaluates the proposed SAG-EERAO model against the Coherent Ising Machine-based Resource Allocation (CIM-RA) framework, as described in [27]. Both models are implemented in the NS3-based SIMITS simulator [31], which supports real-time spectrum access, failure monitoring, and dynamic mobility modeling. To emulate realistic wireless environments, the SUI channel fading model from NYUSIM [32] is adopted to validate MIMO-NOMA network performance, whereas the simulation scenarios are aligned with the DeepMIMO dataset framework [33]. Urban and highway mobility patterns are used to reflect high-speed vehicular movement, capturing the challenges posed by dynamic wireless environments. The 5G propagation behavior follows the setup presented in [22].

To comprehensively evaluate performance, simulations are conducted using a Monte Carlo approach with varying MT densities. Key metrics include throughput, energy consumption, and resource access success rate. To ensure the validity and reproducibility of results, specific attention is paid to the selection of simulation parameters. Power allocation coefficients and utility function weights in SAG-EERAO are fine-tuned through sensitivity analysis to balance efficiency, throughput, and fairness, giving higher priority to weaker users under imperfect SIC.

A detailed parameter list, including channel gain thresholds, SIC sensitivity, and energy limits per MT, is provided in Table I. The parameters reflect real-world 5G deployment standards and align with prior simulation setups used in [22], [27], and [31]. For robustness, the system is evaluated under two scales, 25 and 50 MTs, to observe the sensitivity of throughput, energy utilization, and resource access success across mobility variations.

TABLE I. SIMULATION PARAMETERS

Parameter	Value(s)	Justification
Number of MTs	25, 50	Chosen to reflect small-to-moderate density user scenarios in urban-highway macro-cell environments; evaluated to observe behavior under scaled mobility.
Total bandwidth	5.0 MHz	Commonly used in small-cell and NOMA-based 5G studies; enables fair comparison with prior models [22, 27].
Minimum data rate per user	2 bps/Hz	Ensures QoS requirement per user; aligns with minimum throughput benchmarks in NOMA studies.
Cell radius	500 m	Reflects typical microcell deployment range in 5G MIMO-NOMA urban-highway scenarios.
Minimum distance (user to BS)	50 m	Avoids near-field effects and ensures realistic channel propagation modeling as per SUI model.
Max number of multiplexed users	2 users	Adheres to standard NOMA constraint to avoid excessive inter-user interference [27, 32].
Noise power spectral density	-170 dBm/Hz	Standardized value in 5G simulation environments; used in NYUSIM and SUI-based fading models.
Power allocation coefficients	[0.2–0.8] (dynamic)	Assigned dynamically based on channel gain to ensure fairness and improve throughput under SIC decoding.
Utility function weights ($\omega_1 - \omega_3$)	ω_1=0.4, ω_2=0.3, ω_3=0.3	Selected after empirical tuning to balance throughput (ω_1), energy efficiency (ω_2), and fairness (ω_3).
Channel fading model	SUI from NYUSIM [32]	Captures real-world multipath fading effects for outdoor 5G urban-highway scenarios.
Mobility model	Urban and highway	Represents vehicular mobility; selected to evaluate robustness under varying speeds and high-speed terminal movement.
Monte Carlo iterations	100 per configuration	Ensures statistical significance in observed metrics across variable terminal positioning.
SIC error rate	5%–10% (simulated)	Reflects non-ideal SIC conditions due to imperfect channel estimation, as observed in practical deployments.
CSI imperfection	±10% estimation error	Models realistic feedback conditions; impacts power and resource allocation precision.
Simulation tool	SIMITS (NS3-based) [31]	Enables real-time spectrum access modeling and live terminal failure scenarios.

A. *Throughput Performance*

This section studies the throughput performance of both SAG-EERAO and CIM-RA considering MT sizes of 25 and 50. The throughput is measured as the total number of packets transmitted per channel, expressed in bit/Hz/s, where a higher value indicates better performance. Figure 3 shows the throughput performance of both CIM-RA and SAG-EERAO for 25 MTs. Similarly, Figure 4, shows the throughput performance for 50 MTs. The proposed SAG-EERAO model achieves higher throughput compared to CIM-RA for both 25 and 50 MTs. An average throughput enhancement of 23.39% is observed for 25 MTs and 14.13% for 50 MTs.

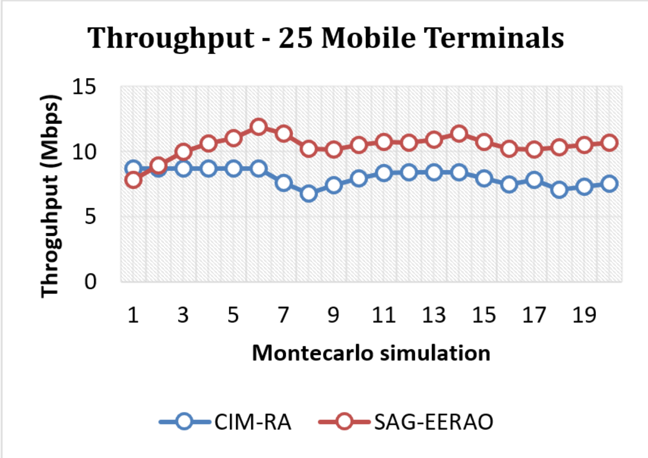

Fig. 3. Throughput performance of SAG-EERAO and CIM-RA for 25 MTs.

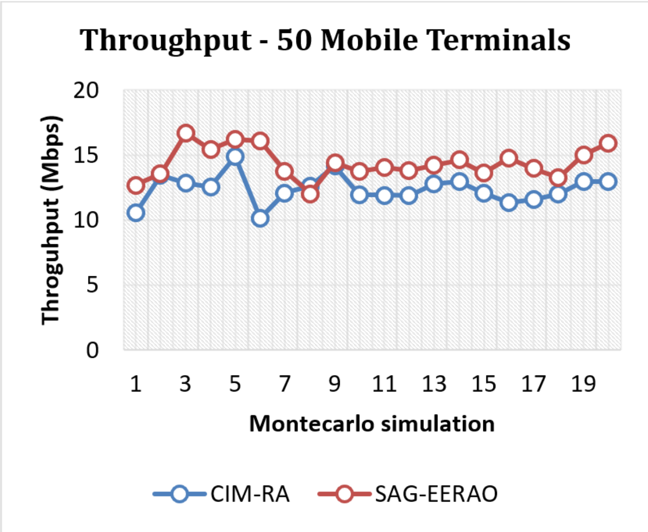

Fig. 4. Throughput performance of SAG-EERAO and CIM-RA for 50 MTs.

B. *Energy Utilization Performance*

This section studies the spectrum access energy usage of both SAG-EERAO and CIM-RA considering MT sizes of 25 and 50. The spectrum access energy usage is measured as the total energy consumed (J) on a given spectrum, where a lower value indicates better performance. Figure 5 shows the spectrum access energy usage of both CIM-RA and SAG-EERAO for 25 MTs. Similarly, Figure 6 shows the spectrum access energy usage for 50 MTs. The proposed SAG-EERAO model reduces spectrum access energy usage compared to CIM-RA for both 25 and 50 MT sizes. An average energy reduction of 70.83% is observed for 25 MTs, and 38.18% for 50 MTs.

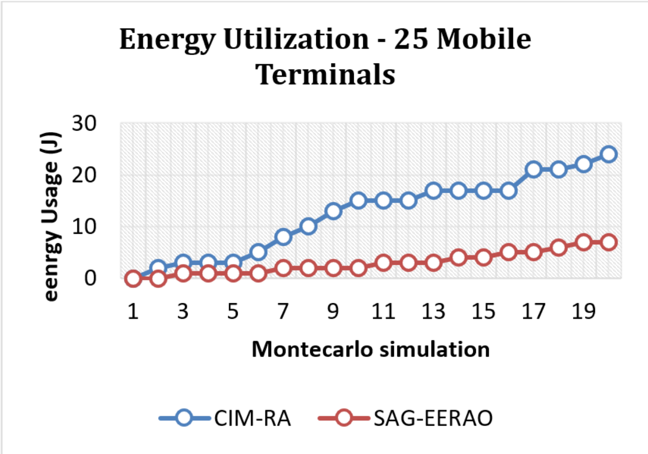

Fig. 5. Energy utilization of SAG-EERAO and CIM-RA for 25 MTs.

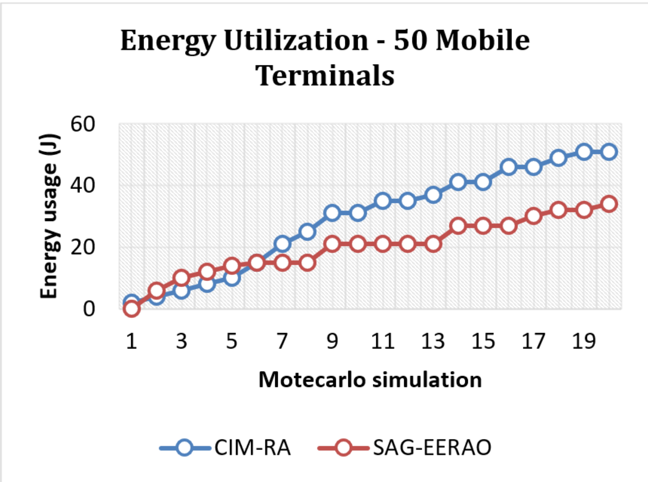

Fig. 6. Energy utilization of SAG-EERAO and CIM-RA for 50 MTs.

C. Resource Access Success Performance

This section studies the resource access success of both SAG-EERAO and CIM-RA for MT sizes of 25 and 50. The resource access success is measured as the total number of successful packet transmissions, where a higher value indicates better performance. Figure 7 shows the resource access success performance of both CIM-RA and SAG-EERAO for 25 MTs. Similarly, Figure 8, shows the resource access success performance for 50 MTs. The proposed SAG-EERAO model achieves higher resource access success compared with CIM-RA for both 25 and 50 MTs. An average resource access success enhancement of 28.81% is observed for 25 MTs, 18.47% for 50 MTs.

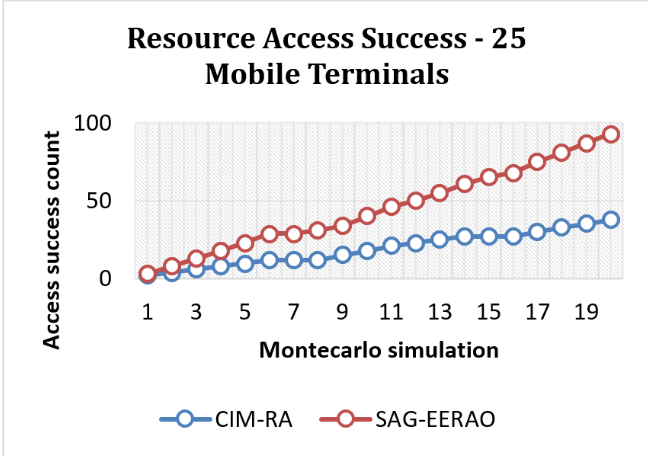

Fig. 7. Resource access success performance of SAG-EERAO and CIM-RA for 25 MTs.

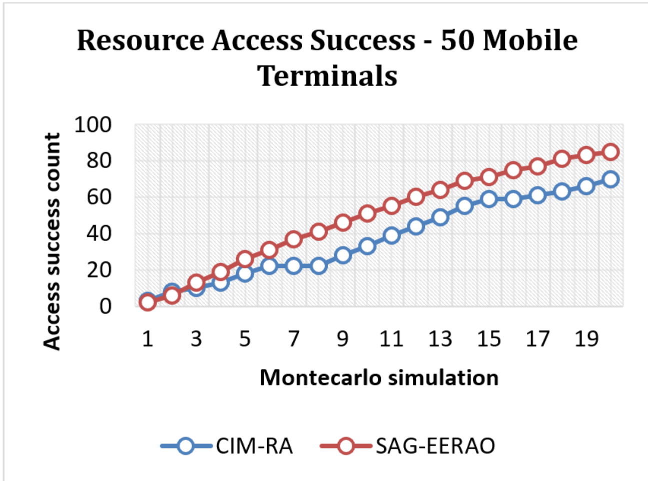

Fig. 8. Resource access success performance of SAG-EERAO and CIM-RA for 50 MTs.

D. Computational Complexity

The proposed SAG-EERAO model achieves efficient resource and user selection through a utility-driven SAG, reducing unnecessary computations. Its complexity is approximately $O(N \cdot M \cdot I)$, with N MTs, M resource units, and I convergence iterations. Unlike [27], which utilizes a CIM and incurs higher quantum-inspired hardware overhead and complexity in encoding optimization problems, SAG-EERAO operates in a standard simulation environment without special hardware dependency. Thus, SAG-EERAO offers better scalability and real-time applicability for large-scale MIMO-NOMA networks, especially under dynamic and mobile urban-highway conditions.

IV. CONCLUSION

This study introduces a new downlink Multiple-Input Multiple-Output Non-Orthogonal Multiple Access (MIMO-NOMA) framework and systematically compares its efficiency with existing conventional resource allocation systems. This work proposes the State-Action Game-based Energy Efficient Resource Allocation Optimization (SAG-EERAO) model, a utility-aware, SAG-based resource allocation approach tailored for fast-varying multipath urban-highway MIMO-NOMA environments. Unlike traditional schemes or Coherent Ising Machine (CIM)-based algorithms, SAG-EERAO introduces adaptive Signal-to-Interference-plus-Noise Ratio (SINR)-aware user selection and dynamic power adjustment with cooperative behavior modeling.

The model's novelty lies in jointly optimizing throughput and power via state-action utility functions under realistic channel variations. Experimental results for 25 and 50 Mobile Terminals (MTs) show that SAG-EERAO outperforms CIM-RA in throughput (by up to 54.5%), energy efficiency (by 18.76%), and spectrum utilization (by 23.64%). These results demonstrate SAG-EERAO's scalability and applicability in 6G-enabled dense mobile scenarios.

Although the simulation results confirm the efficacy of the SAG-EERAO model, further investigation under real-world constraints is essential to validate its deployment potential. In this regard, the simulation framework accounts for dynamic topology changes, MT mobility, and non-ideal channel feedback to approximate real deployment conditions. Nonetheless, an in-depth analysis of the model's behavior under varying mobility patterns (e.g., urban vs. rural), rapid user density fluctuations, and complex handover scenarios would provide further insight into its scalability and robustness. Moreover, future work should consider the computational complexity of SAG-EERAO in large-scale network deployments. Preliminary runtime analysis indicates that while SAG-EERAO converges faster than brute-force optimization techniques, its integration with lightweight Deep Reinforcement Learning (DRL) or hardware-accelerated scheduling may be required for real-time implementation in ultra-dense network scenarios.

ACKNOWLEDGMENT

We would like to express our sincere gratitude to all those who have supported and contributed to this research project. In particular, we extend our heartfelt thanks to our guide for his unwavering guidance, invaluable insights, and encouragement throughout the research process. No funding was raised for this research.

REFERENCES

[1] G. Verma and S. T. Ali, "Non-Orthogonal Multiple Access (NOMA) for 5G Wireless Networks: A Performance Evaluation," *International Journal of Sciences and Innovation Engineering*, vol. 2, no. 1, pp. 7–14, Jan. 2025, https://doi.org/10.70849/IJSCI.

[2] Y. Liu, Z. Qin, M. Elkashlan, Z. Ding, A. Nallanathan, and L. Hanzo, "Nonorthogonal Multiple Access for 5G and Beyond," *Proceedings of the IEEE*, vol. 105, no. 12, pp. 2347–2381, Dec. 2017, https://doi.org/10.1109/JPROC.2017.2768666.

[3] W. Jiang, Z. Teng, Q. Wang, and L. Qian, "Time Division Multiple Access–Non-Orthogonal Multiple Access-Assisted Heterogeneous Semantic and Bit Communications," *Electronics*, vol. 14, no. 5, Mar. 2025, Art. no. 1005, https://doi.org/10.3390/electronics14051005.

[4] A. Nasser, A. Celik, and A. M. Eltawil, "Joint User-Target Pairing, Power Control, and Beamforming for NOMA-Aided ISAC Networks," *IEEE Transactions on Cognitive Communications and Networking*, vol. 11, no. 1, pp. 316–332, Feb. 2025, https://doi.org/10.1109/TCCN.2024.3427781.

[5] N. K. Breesam, W. A. Al-Hussaibi, F. H. Ali, and I. M. Al-Musawi, "Efficient Resource Allocation for Wireless-Powered MIMO-NOMA Communications," *IEEE Access*, vol. 10, pp. 130302–130313, 2022, https://doi.org/10.1109/ACCESS.2022.3228754.

[6] H. Vidyaningtyas, Iskandar, Hendrawan, and A. A. Pramudita, "NOMA Performance Improvement with Downlink Sectorization," *Emerging Science Journal*, vol. 9, no. 1, pp. 311–328, Feb. 2025, https://doi.org/10.28991/ESJ-2025-09-01-017.

[7] S. Bisen, V. Bhatia, and P. Brida, "Successive interference cancellation with multiple feedback in NOMA-enabled massive IoT network," *EURASIP Journal on Wireless Communications and Networking*, vol. 2024, no. 1, Sep. 2024, Art. no. 71, https://doi.org/10.1186/s13638-024-02404-1.

[8] Z. Hu, C. Han, Y. Deng, and X. Wang, "Multi-Task Deep Reinforcement Learning for Terahertz NOMA Resource Allocation With Hybrid Discrete and Continuous Actions," *IEEE Transactions on Vehicular Technology*, vol. 73, no. 8, pp. 11647–11663, Aug. 2024, https://doi.org/10.1109/TVT.2024.3381238.

[9] G. Wu, G. Chen, and X. Gu, "Multi-agent learning based UAV-assisted MEC-NOMA for cellular offloading in Internet of Things," *Expert Systems with Applications*, vol. 270, Apr. 2025, Art. no. 126567, https://doi.org/10.1016/j.eswa.2025.126567.

[10] K. Selvam and K. Kumar, "Energy-aware resource allocation in machine to machine system-based NOMA using hybridized shark smell with lemur's optimization," *Telecommunication Systems*, vol. 88, no. 1, Jan. 2025, Art. no. 24, https://doi.org/10.1007/s11235-024-01258-8.

[11] D. R and V. B. Kumaravelu, "Outage analysis and power optimization in uplink and downlink NOMA systems with Rician fading," *Results in Engineering*, vol. 25, Mar. 2025, Art. no. 104021, https://doi.org/10.1016/j.rineng.2025.104021.

[12] N. Omheni, A. Amiri, and F. Zarai, "A detailed reinforcement learning framework for resource allocation in non-orthogonal multiple access enabled-B5G/6G networks," *IET Networks*, vol. 13, no. 5–6, pp. 455–470, Sep. 2024, https://doi.org/10.1049/ntw2.12131.

[13] M. K. Tefera, S. Zhang, and Z. Jin, "Deep Reinforcement Learning-Assisted Optimization for Resource Allocation in Downlink OFDMA Cooperative Systems," *Entropy*, vol. 25, no. 3, Mar. 2023, Art. no. 413, https://doi.org/10.3390/e25030413.

[14] J. Li, T. Gao, B. He, W. Zheng, and F. Lin, "Power Allocation and User Grouping for NOMA Downlink Systems," *Applied Sciences*, vol. 13, no. 4, Feb. 2023, Art. no. 2452, https://doi.org/10.3390/app13042452.

[15] Y. P. Santos and L. F. Q. Silveira, "Adaptive Clustering of Users in Power Domain NOMA," *Sensors*, vol. 23, no. 11, Jun. 2023, Art. no. 5314, https://doi.org/10.3390/s23115314.

[16] Q. Alghazali, H. Al-Amaireh, and T. Cinkler, "Joint Power and Channel Allocation for Non-Orthogonal Multiple Access in 5G Networks and Beyond," *Sensors*, vol. 23, no. 19, Oct. 2023, Art. no. 8040, https://doi.org/10.3390/s23198040.

[17] H. Rajab, B. Ren, and T. Cinkler, "A Novel Approach to Enhance the Energy Efficiency of a NOMA Network," *Telecom*, vol. 4, no. 3, pp. 611–628, Sep. 2023, https://doi.org/10.3390/telecom4030027.

[18] J. Ding, L. Han, J. Li, and D. Zhang, "Resource allocation strategy for blockchain-enabled NOMA-based MEC networks," *Journal of Cloud Computing*, vol. 12, no. 1, Oct. 2023, Art. no. 142, https://doi.org/10.1186/s13677-023-00497-5.

[19] P. Lai *et al.*, "Online User and Power Allocation in Dynamic NOMA-Based Mobile Edge Computing," *IEEE Transactions on Mobile Computing*, vol. 22, no. 11, pp. 6676–6689, Nov. 2023, https://doi.org/10.1109/TMC.2022.3193366.

[20] P. Tennakoon, S. Rajkumar, and D. N. K. Jayakody, "Game Theory Based Delta-OMA Scheme for VLC Networks," *IEEE Access*, vol. 11, pp. 10777–10791, 2023, https://doi.org/10.1109/ACCESS.2023.3240065.

[21] Z. H. Shaik, R. Sarvendranath, and E. G. Larsson, "Energy-Efficient Resource Allocation for Underlay Spectrum Sharing in Cell-Free Massive MIMO," *IEEE Access*, vol. 12, pp. 106895–106911, 2024, https://doi.org/10.1109/ACCESS.2024.3432287.

[22] J. Ji, X. Ren, L. Cai, and K. Zhu, "Downlink Scheduler for Delay Guaranteed Services Using Deep Reinforcement Learning," *IEEE Transactions on Mobile Computing*, vol. 23, no. 4, pp. 3376–3390, Apr. 2024, https://doi.org/10.1109/TMC.2023.3276697.

[23] S. Amin, J. A. Sheikh, Mehboob-ul-Amin, and B. A. Malik, "A deep reinforcement learning for energy efficient resource allocation Intelligent Reflecting Surface (IRS) driven Non-Orthogonal Multiple Access Beamforming (NOMA-BF)," *Physical Communication*, vol. 60, Oct. 2023, Art. no. 102148, https://doi.org/10.1016/j.phycom.2023.102148.

[24] X. Wang, Y. Wang, J. Zhao, C. Weng, Y. Yan, and Z. Li, "Joint Long-Term User Scheduling and Beamforming Design for Burst IIoT," *IEEE Internet of Things Journal*, vol. 11, no. 12, pp. 22628–22642, Jun. 2024, https://doi.org/10.1109/JIOT.2024.3382738.

[25] Z. Tao, W. Xu, and X. You, "Digital Twin-Accelerated Online Deep Reinforcement Learning for Admission Control in Sliced Communication Networks," *IEEE Transactions on Communications*, vol. 73, no. 4, pp. 2490–2504, Apr. 2025, https://doi.org/10.1109/TCOMM.2024.3476430.

[26] M. Ahmadi, A. Moayyedi, M. Sulaiman, M. A. Salahuddin, R. Boutaba, and A. Saleh, "Generalizable 5G RAN/MEC Slicing and Admission Control for Reliable Network Operation," *IEEE Transactions on Network and Service Management*, vol. 21, no. 5, pp. 5384–5399, Oct. 2024, https://doi.org/10.1109/TNSM.2024.3437217.

[27] T. Otsuka, A. Li, H. Takesue, K. Inaba, K. Aihara, and M. Hasegawa, "High-Speed Resource Allocation Algorithm Using a Coherent Ising Machine for NOMA Systems," *IEEE Transactions on Vehicular Technology*, vol. 73, no. 1, pp. 707–723, Jan. 2024, https://doi.org/10.1109/TVT.2023.3300920.

[28] A. Gholamrezaee, H. Farrokhi, and J. Z. Moghaddam, "Fair resource allocation and SBS selection for MC-NOMA-based HetNets supporting D2D communications," *Physical Communication*, vol. 63, Apr. 2024, Art. no. 102297, https://doi.org/10.1016/j.phycom.2024.102297.

[29] P. Gupta, A. Kumar, and R. Sharma, "Resource allocation method for improved spectral efficiency, outage probability and user fairness in NOMA," *International Journal of Electronics*, vol. 112, no. 3, pp. 391–410, Mar. 2025, https://doi.org/10.1080/00207217.2024.2302340.

[30] A. Shabbir, H. R. Khan, S. A. Ali, and S. Rizvi, "Design and Performance Analysis of Multi-tier Heterogeneous Network through Coverage, Throughput and Energy Efficiency," *Engineering, Technology & Applied Science Research*, vol. 7, no. 6, pp. 2345–2350, Dec. 2017, https://doi.org/10.48084/etasr.1256.

[31] N. Gadde, B. Jakkali, R. B. H. Siddamallaih, and G. Gowrishankar, "Quality of experience aware network selection model for service provisioning in heterogeneous network," *International Journal of Electrical and Computer Engineering*, vol. 12, no. 2, pp. 1839–1848, Apr. 2022, https://doi.org/10.11591/ijece.v12i2.pp1839-1848.

[32] A. Mahmood, S. Khan, S. Hussain, and M. Zeeshan, "Performance Analysis of Multi-User Downlink PD-NOMA Under SUI Fading Channel Models," *IEEE Access*, vol. 9, pp. 52851–52859, 2021, https://doi.org/10.1109/ACCESS.2021.3070147.

[33] T. H. Ahmed, J. J. Tiang, A. Mahmud, C. Gwo-Chin, and D.-T. Do, "Proposed CtCNet-HDRNN: A Cornerstone in the Integration of 5G mmWave and DSRC for High-Speed Vehicular Networks," *IEEE Access*, vol. 11, pp. 126482–126506, 2023, https://doi.org/10.1109/ACCESS.2023.3329872.